

Liquid pressure sensing system based on distributed polarization crosstalk analysis in polarization maintaining fiber*

HE Zongjiang¹, ZHANG Zeheng¹, FENG Ting^{1**}, LI Qing¹, and YAO X Steve^{1,2}

1. Photonics Information Innovation Center and Hebei Provincial Center for Optical Sensing Innovations, College of Physics Science & Technology, Hebei University, Baoding 071002, China

2. NuVision Photonics, Inc., Las Vegas 89109, USA

(Received 29 April 2022; Revised 28 June 2022)

©Tianjin University of Technology 2022

A novel quasi-distributed liquid pressure sensing system based on distributed polarization crosstalk analysis (DPXA) in polarization maintaining fiber (PMF) is proposed and demonstrated. We design a special structure of liquid pressure sensing units and invent a corresponding nonlinear calibration method. Five sensing units deployed on a sensing tape can effectively transform the liquid pressure into the transverse-force applied on the sensing PMF, and the induced polarization crosstalk can be measured and located by the DPXA system, so as to further establish the relationship between liquid pressure and crosstalk through the nonlinear calibration method. The liquid pressure sensing system has good sensitivity and high repeatability, and a maximal measurement relative error of 8.96% is measured for the five sensing units, which can be much improved by optimizing the packaging of sensing units. We believe our sensing system will find great applications in the field of engineering liquid pressure sensing.

Document code: A **Article ID:** 1673-1905(2022)11-0651-7

DOI <https://doi.org/10.1007/s11801-022-2072-z>

Depth-resolved liquid pressure is a very important parameter for large industry liquid storage tank management, healthy monitoring of water conservancy facilities, petroleum and natural gas exploitation and liquid stratification detection^[1]. However, traditional electrical pressure sensor is difficult to satisfy the requirements of industrial engineering, especially in complex environments, due to its live line work mode and discrete measurement characteristic. Distributed optical fiber sensing (DOFS) technique has been paid broad attention in industrial engineering sensing field in recent years by means of its merits of small in size, electric insulation, high temperature resistance, corrosion resistance and position-resolved sensing capability^[2-6]. What's more, DOFS for liquid pressure or liquid depth measurement has also made lots of progresses. There are mainly two types of fiber sensors to measure liquid pressure or liquid depth (or level). The first one is based on the interaction between ambient conditions and optical field, and the most representative one is the fiber Mach-Zehnder interferometer. In 2014, GONG et al^[7] proposed a modal interferometer based on polarization maintaining fiber (PMF) to sense liquid level, and its sensitivity achieves 279 pm/mm. However, this type of fiber sensor is sus-

ceptible to temperature and its spatial sensing range is quite limited. The other type is based on converting the measurement of external liquid pressure to the measurement of fiber strain, since most fiber sensors are insensitive to transverse pressure, such as optical backscattered reflectometer^[8] and fiber Bragg grating^[9]. SCHENATO et al^[10] reported a liquid pressure sensing probe in 2016, and the main effort made is improving the low pressure sensitivity of optical fiber and coping with the cross-sensitivity to temperature. They proposed a dual-chamber fiber probe whose chambers have different behaviors under pressure and temperature influences, thus by demodulating the differential strain induced in two chambers, both pressure and temperature information can be obtained. The liquid pressure resolution of the proposed probe achieves 0.3 kPa, but this method can not realize depth-resolved sensing. In 2020, they came up with a new liquid pressure sensing unit, in which two D-shape rubber slabs were used to constitute the stress-strain converter and the sensing fiber was affixed on the inner surface of the D-shape rubber slab in a zig-zag shape^[11]. Its sensitivity and accuracy were respectively 30 GHz/kPa and 1 kPa. However, its capability to measure the continuously changing liquid pressure along

* This work has been supported by the National Natural Science Foundation of China (Nos.61975049 and 51777051), the Science Fund for Distinguished Young Scholars of Hebei Province (No.F2020201001), the Science and Technology Research Project of Colleges and Universities in Hebei Province (No.ZD2022138), and the Hebei Provincial Innovation Ability Promotion Project (No.20542201D).

** E-mail: wlxft@hbu.edu.cn

the depth direction was not validated.

To achieve the depth-resolved liquid-pressure measurement, we want to introduce the PMF based distributed polarization crosstalk analysis (DPXA) technique^[12,13] to realize liquid pressure sensing. The DPXA has been proved owning outstanding transverse-force (TF) sensing capability, with cm-level resolution and km-level measurement distance^[12,13]. In addition, unlike other fiber sensing techniques based on the stress-to-strain conversion, the DPXA can directly obtain the TF information by means of measuring the force-induced polarization crosstalk along the PMF. Besides, although the DPXA technique is sensitive to temperature^[14], the measurements of TF and temperature are orthogonal and independent^[15,16].

In this letter, we report a quasi-distributed liquid pressure sensing system based on the DPXA, using a specially designed sensing tape with multiple sensing units. The sensing units can convert liquid pressure to TF applied on the PMF effectively. Moreover, a nonlinear calibration method is proposed accordingly which establishes the relationship between the liquid pressure and the polarization crosstalk for every sensing unit. Our system has the advantages of high sensitivity and large measurement dynamic range, which enable it to be with good potential in depth-resolved liquid pressure sensing applications.

The structure of the liquid pressure sensing system based on the DPXA system is shown in Fig.1.

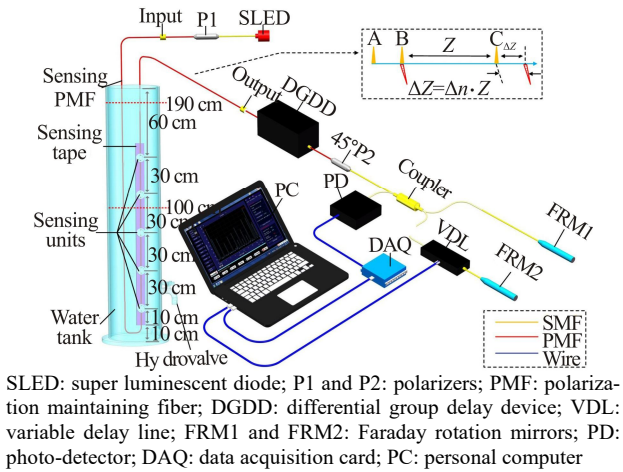


Fig.1 Illustration of liquid pressure sensing system based on a ghost-peak-free DPXA system

The DPXA system is constructed based on a scanning white light Michelson interferometer, whose working principle can be simply described as follows (as illustrated in the inset of Fig.1). The probe light emitted by a super luminescent diode (SLED), centered at 1 550 nm with a coherence length $\sim 25 \mu\text{m}$ (corresponding to a 3-dB Gaussian linewidth of $\sim 30 \text{ nm}$), is polarized by a polarizer P1 and enters the sensing PMF along the slow axis at the input point (A). When the PMF is perturbed

by an external TF at a certain point (B), a part of the probe light along the slow axis will couple into the fast axis. Because the propagation constants of fast axis and slow axis are different, the two light components will have a certain optical path difference ΔZ when they together propagate a fiber distance Z to reach the output point (C) of PMF, and we can obtain the relationship as

$$\Delta Z = Z \times \Delta n, \quad (1)$$

where Δn is the birefringence of the PMF. After outputting from the sensing PMF, the two light components are projected to the same polarization state through a polarizer (P2) with the transmission polarization principal axis 45° oriented with the slow axis of the PMF, and then interfere in the white light Michelson interferometer by changing the delay value (D_L) introduced in one of the two arms via a variable delay line (VDL) to compensate the optical path difference ΔZ . Here, we get the D_L equal to the optical path difference ΔZ . Subsequently, by analyzing the interference pattern and according to Eq.(1), the intensity of TF-induced polarization crosstalk and the TF position (point B) can be obtained. It should be noted that, when there are several TFs applied to the sensing PMF, the iterative optical couplings between slow and fast axes will lead to the appearance of ghost peaks. In order to eliminate the influence of ghost peaks, a differential group delay device (DGDD) is installed behind the output end of PMF to add a sufficient delay difference between the orthogonal polarization light components^[12,13], which enable the DPXA to unambiguously and accurately identify every polarization crosstalk along the sensing PMF.

The polarization crosstalk intensity in a PMF can be defined as^[17,18]

$$h = F^2 \times \sin^2(2\alpha) \times \left\{ \frac{\sin \left[\pi \sqrt{1 + F^2 + 2F \cos(2\alpha)} (l/L_{b0}) \right]}{\sqrt{1 + F^2 + 2F \cos(2\alpha)}} \right\}^2, \quad (2)$$

where $\alpha=45^\circ$ is the angle between the TF and the slow axis of the PMF, $l \approx 0.5 \text{ mm}$ is the TF-applying length, $L_{b0}=2.32 \text{ mm}$ is the beat length, and F is the normalized force defined as

$$F = \frac{5458.6 L_{b0}}{r \lambda} f, \quad (3)$$

where f is TF (line-force) value, $r=62.5 \mu\text{m}$ is the fiber radius, and $\lambda=1550 \text{ nm}$ is the center wavelength of SLED.

The liquid pressure sensing tape was made by glue-fixing five sensing units (from No.1 to No.5) on a steel ruler with an adjacent distance of 30 cm. The structure of the sensing unit is shown by the disassembly view in Fig.2, mainly composed of a base sheet, the sensing PMF, a pressing sheet, a silicone film, a seal ring and a seal sheet, from bottom to top. The base sheet and seal sheet were made by the 3-D printer using resin material. The base sheet has a circular hole channel with a diameter

of 1 mm for the sensing fiber to pass through, and the corresponding position of the seal sheet is hollowed with a circular groove to avoid introducing extra pressure on the fiber. The PMF is fixed on the inner surface of the base sheet with UV glue and the passing hole is sealed by waterproof glue. The pressure induced TF is applied on the PMF through a pressing sheet, three metal rods and a piece of silicone film. The pressing rod on the sensing PMF transmits the TF to the fiber, and the two supporting rods on two segments of supporting PMFs keep balance of the pressing sheet. The silicone film has good ductility and water proof property, whose edge is tightly pressed in the groove of the base sheet by the seal ring and clamped by the base sheet and the seal sheet. Eight screw holes are deployed correspondingly on the base sheet and seal sheet to integrate all of the components to a whole with screws. It is worth noting that according to Eq.(2), the crosstalk intensity h is closely related to α . In order to ensure a high sensitivity of the sensing unit, the PMF was rotated to seek the optimal radial direction of the slow axis before the packaging.

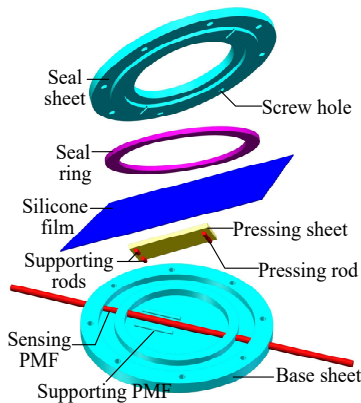


Fig.2 Disassembly view of the sensing unit

For implementing the quasi-distributed liquid pressure sensing, the relationship of crosstalk versus pressure must be obtained for each sensing unit. We custom-made a cylinder water tank with a height of 200 cm and fixed the sensing tape on its inner surface, as shown in Fig.1. The sensing unit 1 is fixed 10 cm away from the bottom of the sensing tape, and the bottom of the sensing tape is 10 cm away from the bottom of the water tank. In order to simulate the change of liquid pressure for every sensing unit, we changed the water level by injecting water from the hole of the water tank top or discharging water from the hydrovalve. The distributed polarization crosstalk curves along the sensing PMF were measured with water levels of 100 cm and 190 cm respectively in the water tank, as shown in Fig.3. The crosstalk peaks marked as No.1 to No.5 correspond to the five sensing units on the sensing tape, and different sensing units are subjected to different pressures at different water depths to induce crosstalk peaks with different heights. The crosstalk peak between sensing units 1 and 2 is caused by the stress from fiber fixing on the sensing tape using the sellotape. In addition, according to the results in

Fig.3, it can be known that the radial uniform stress from the water applied to the PMF outside the five sensing units cannot induce polarization crosstalk. Note that, due to the low repeatability of handwork packaging, the original crosstalk intensities of five sensing units without applying pressure were different.

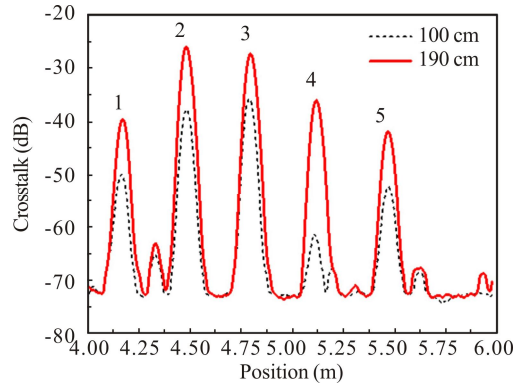


Fig.3 Distributed crosstalk measurement along the sensing PMF with different water levels of 100 cm and 190 cm of the water tank

We change the water level from 100 cm to 190 cm and from 190 cm to 100 cm, respectively, with a depth variation of 10 cm each time. The measured crosstalk values for five sensing units are shown in Fig.4(a) to Fig.4(e), respectively. Since the sensing units 1 to 3 are always under the water level while the sensing units 4 and 5 gradually sink into or emerge from the water at the depth of 110 cm and 150 cm respectively, we can investigate the crosstalk variation processes for different measurement states. The crosstalk distribution curves were measured after the water level stabilized for 5 min for each depth variation, and at each level 10 times measurements were carried out and averaged to reduce the random errors. As can be seen in Fig.4, all of the sensing units work well and have a very good repeatability for water level increase and decrease. However, due to the handwork packaging induced different original crosstalk values and sensing sensitivity deviations for five sensing units, their sensing effects seem quite different from each other. In addition, obvious nonlinearity between crosstalk and water level can be seen for sensing units 1, 4 and 5. Therefore, a nonlinear calibration for each sensing unit must be implemented for achieving accurate sensing of our system, similar to that of most fiber optic sensing systems reported in literatures.

The theory in Eq.(2) gives the relationship between crosstalk h and line-force f . Theoretically, a water level L corresponds to a line-force f with a fixed conversion coefficient c for each sensing unit, but five sensing units are with different conversion coefficients due to the limit of handwork packaging. For achieving the calibration of sensing relationship between crosstalk and water level, we must obtain the conversion coefficient between water level and line-force for every sensing unit according to the theory. We develop the following method for calibration, and take sensing unit 1 as an example, as shown in

Fig.5. We define Δf as a line-force interval corresponding to the water level changing step of 10 cm used for experiments, h_1 to h_{10} as the crosstalk values respectively at the water levels used in experiments from 100 cm to 190 cm with a changing step ΔL of 10 cm, and carry out the following processes.

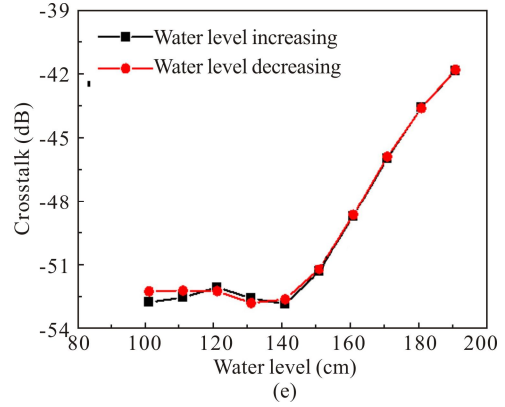
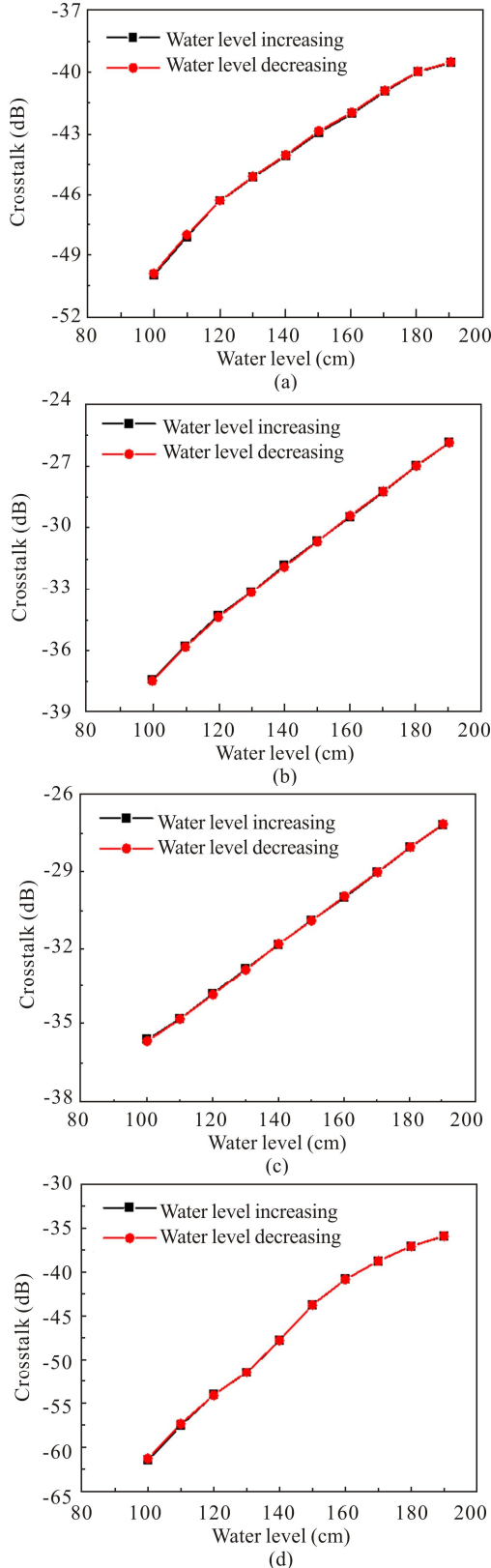


Fig.4 Polarization crosstalk values measured for sensing units (a) 1, (b) 2, (c) 3, (d) 4, and (e) 5, respectively, when the water level increasing from 100 cm to 190 cm and decreasing from 190 cm to 100 cm

(1) Substituting the measured first crosstalk value defined as h_1 at the initial water depth L_1 ($L_1=100$ cm for sensing unit 1) into Eq.(2) to calculate the corresponding line-force f_1 , and defining the (f_1, h_1) as the starting point for calibration.

(2) Plotting the theoretical curve of crosstalk h versus line-force f , and obtaining a series of points $(f_1+\Delta f, h_2')$, $(f_1+2\Delta f, h_3')$, $(f_1+3\Delta f, h_4')$, ..., $(f_1+9\Delta f, h_{10}')$ from the curve.

(3) Defining a fitting residual S to denote the difference between experimental data and corresponding points obtained in process (2), and calculating it as

$$S = (h_2 - h_2')^2 + (h_3 - h_3')^2 + \dots + (h_{10} - h_{10}')^2. \quad (4)$$

(4) Numerical calculating and plotting the relationship between S and Δf , as shown in Fig.6, and finding the Δf corresponding to the minimum S , which provides the best fit between the experiment and theory.

(5) Establishing the relationship between water level L and line-force f as

$$L = \frac{(f - f_1)}{c} + L_1. \quad (5)$$

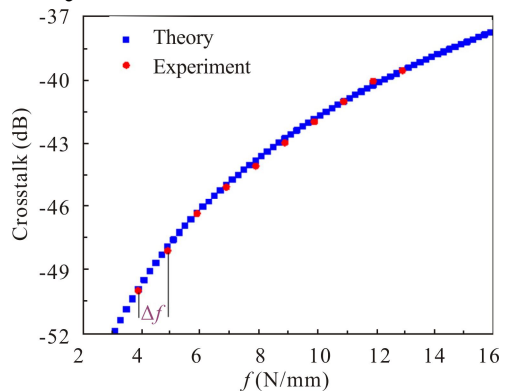


Fig.5 Fitting result of experimental data and theoretical curve for sensing unit 1

For sensing unit 1, $f_1=3.866$ N/mm is obtained in Fig.5, $\Delta f=1$ N/mm is obtained in Fig.6 (marked as the red

point), and $c=0.10$ N/mm/cm is calculated as $c=\Delta f/\Delta L$. Therefore, we can obtain the calibrated relationship between water level L and line-force f as $L=10(f-3.866)+100$ for sensing unit 1, and plot the measured crosstalk values in Fig.5. As can be seen, the experiment and theory agree well with each other. Using the above method, a calibration for every sensing unit can be implemented.

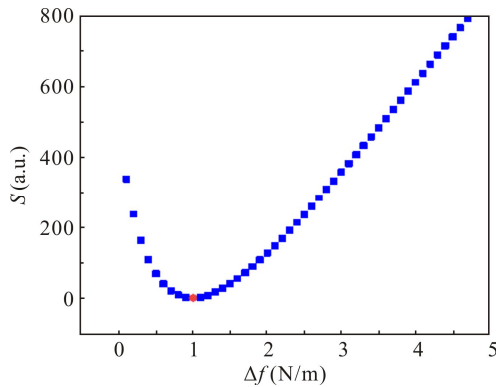


Fig.6 Fitting residual S versus Δf for sensing unit 1

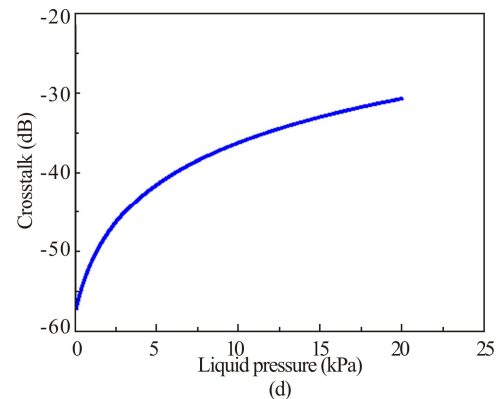
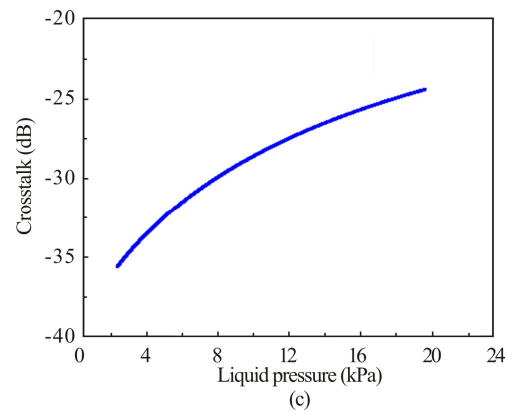
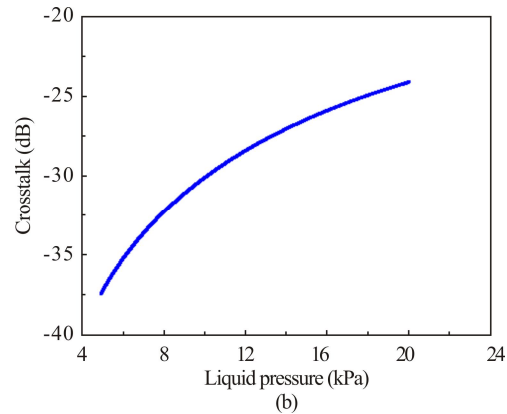
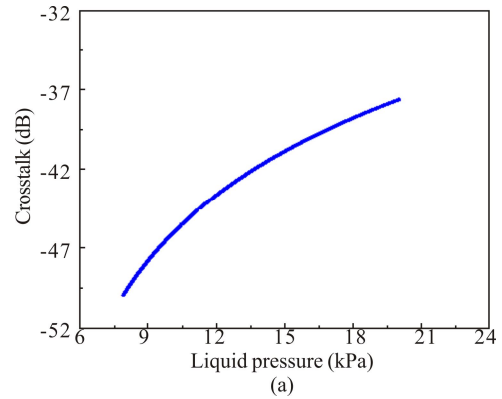
The liquid pressure P can be calculated using

$$P=\rho gH, \tag{6}$$

where $\rho=1$ g/cm³ is the water density, $g=9.8$ N/kg is the gravitational acceleration, and H is the water depth. The water depth H for each sensing unit can be calculated using the position of sensing unit in the water tank as marked in Fig.1 and the water level L measured above. Therefore, according to Eq.(6) and the relationship between the TF liquid pressure obtained by the above calibration method, the relationships of crosstalk versus liquid pressure for all five sensing units are obtained, as shown in Fig.7. The c values of the five sensing units obtained are 0.10 N/mm/cm, 0.43 N/mm/cm, 0.32 N/mm/cm, 0.17 N/mm/cm and 0.12 N/mm/cm, respectively. It can be seen from Fig.7 that the sensing sensitivity cannot be given because the relationship of crosstalk versus liquid pressure for each sensing unit is not linear, and due to the error of handwork packaging, different sensing units have different sensing curves. In addition, according to the theoretical analysis process above and the calibration relationship between the polarization crosstalk and liquid pressure obtained in Fig.7, the crosstalk dynamic-range induced liquid pressure measurement range is 0—135 kPa in theory.

To verify the liquid pressure sensing effect of our sensing system with the above calibration method, we set several water levels of the water tank to simulate different liquid pressures applied to each sensing units and compared the measured pressure values and the corresponding absolute pressures calculated using the real water-depths. In the experiments, the absolute water-depths were read out by a band tape measure. We set five experiments with five water levels for the water tank, and, for each water level, we measured the liquid pres-

ures using the five pressing units respectively. In each experiment, 10 times of repeated measurements were performed and averaged to obtain the pressure value for each sensing unit. The verification experimental results



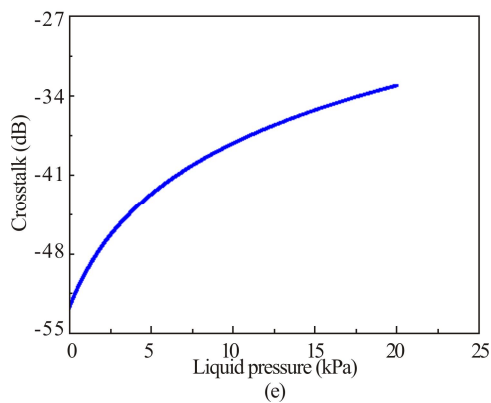


Fig.7 Calibrated relationship between crosstalk and liquid pressure for sensing units (a) 1, (b) 2, (c) 3, (d) 4, and (e) 5

are listed in Tab.1. It can be seen from Tab.1 that the maximum measurement error of five sensing units occurs when the fourth sensing unit senses the liquid pressure of 13.23 kPa, and the error is 1.19 kPa, indicating a maximal relative error of 8.96%. The different errors between different sensing units are mainly due to the low repeatability of handwork packaging of the sensing units, so the next work is to further improve the packaging repeatability and enhance the robustness of the sensing units.

Tab.1 Experimental data of sensing verification

Absolute pressure (kPa)	Measured pressure (kPa)					Maximal error (kPa/%)
	Unit 1	Unit 2	Unit 3	Unit 4	Unit 5	
9.31	9.34	9.37	9.40	-	-	0.09/0.97
11.27	11.29	10.97	10.77	11.02	-	0.50/4.43
13.23	13.04	12.59	12.64	12.04	13.721	1.19/8.96
15.19	15.09	14.81	14.87	15.38	14.66	0.53/3.49
17.15	17.41	17.62	17.60	*	17.24	0.47/2.73

“-” denotes the sensing unit is out of the water;

“*” denotes the sensing unit is measurement-abnormal.

The main factors that cause the sensing error in the verification experiment may include the following factors. (1) System error: the DPXA system’s inherent measurement error is about ± 0.5 dB at -30 dB, obtained by carrying out 100 repeated measurements with a TF induced polarization crosstalk of ~ -30 dB; (2) Calibration error: the experimental data points do not completely coincide with the calibration curve, inducing that the calibration curves have little errors; (3) Absolute water-depth measurement error: the water-depth of each sensing unit located is read out by the band tape measure with an error ~ 0.2 cm; (4) Liquid pressure error: the accurate liquid pressure should be measured using a high precision pressure measurement instrument rather than calculated according to the water depth.

In summary, we demonstrate a quasi-distributed liquid pressure sensing system composed of a DXPA system

and a novel PMF sensing tape. Five sensing units with a specially designed structure are deployed on the sensing tape based on the PMF. By fixing the sensing tape in a water tank and changing the water-level to simulate the liquid pressure changing, we propose a nonlinear calibration method capable of obtaining the calibration curve on the relationship between polarization crosstalk and liquid pressure for every sensing unit. In the calibration experiment, every sensing unit shows good response sensitivity and measurement repeatability, and in the verification experiment the liquid pressure measurement shows good accuracy with a maximal relative error of 8.96%. The results have validated the good feasibility of quasi-distributed liquid pressure sensing of our sensing system, and its performance can be much improved by optimizing the packaging technique and further reducing the measurement errors, expanding the measurement range and improving the measurement accuracy.

Statements and Declarations

The authors declare that there are no conflicts of interest related to this article.

References

- [1] LAI C W, LO Y L, et al. Application of fiber Bragg grating level sensor and Fabry-Perot pressure sensor to simultaneous measurement of liquid level and specific gravity[J]. IEEE sensors journal, 2012, 12(4): 827-831.
- [2] VERONICA M S, DANIEL L, AITOR L A, et al. Study of optical fiber sensors for cryogenic temperature measurements[J]. Sensors, 2017, 17(12): 2773.
- [3] CHEN X W, ZHANG H X, JIA D G, et al. Implementation of distributed polarization maintaining fiber polarization coupling pressure sensing system[J]. Chinese journal of lasers, 2010, 37(6): 1467-1472.
- [4] LU P, et al. Distributed optical fiber sensing: review and perspective[J]. Applied physics reviews, 2019, 6(4): 041302.
- [5] YU Z, YANG J, LIN C, et al. Distributed polarization measurement for fiber sensing coils: a review[J]. Journal of lightwave technology, 2020, 39(12): 3699-3710.
- [6] BADO M F, et al. A review of recent distributed optical fiber sensors applications for civil engineering structural health monitoring[J]. Sensors, 2021, 21(5): 1818.
- [7] GONG H, SONG H, ZHANG S, et al. An optical liquid level sensor based on polarization-maintaining fiber modal interferometer[J]. Sensors and actuators A: physical, 2014, 205: 204-207.
- [8] VILLALBA S, CASAS J R. Application of optical fiber distributed sensing to health monitoring of concrete structures[J]. Mechanical systems and signal processing, 2013, 39(1-2): 441-451.
- [9] AHMAD H, CHONG W Y, et al. High sensitivity fiber Bragg grating pressure sensor using thin metal diaphragm[J]. IEEE sensors journal, 2009, 9(12): 1654-

- 1659.
- [10] SCHENATO L, ANEESH R, PALMIERI L, et al. Fiber optic sensor for hydrostatic pressure and temperature measurement in riverbanks monitoring[J]. *Optics & laser technology*, 2016, 82: 57-62.
- [11] SCHENATO L, PASUTO A, GALTAROSSA A, et al. An optical fiber distributed pressure sensing cable with pa-sensitivity and enhanced spatial resolution[J]. *IEEE sensors journal*, 2020, 34(12): 5900-5908.
- [12] LI Z, YAO X S, CHEN X, et al. Complete characterization of polarization-maintaining fibers using distributed polarization analysis[J]. *Journal of lightwave technology*, 2014, 33(2): 372-380.
- [13] ZHANG Z, FENG T, LI Z, et al. Experimental study of transversal-stress-induced polarization crosstalk behaviors in polarization maintaining fibers[C]//Advanced Sensor Systems and Applications IX, November 20, 2019, Hangzhou, China. Bellingham: SPIE, 2019: 112-118.
- [14] LI Z H, STENE Y, et al. Research on influence of polarization crosstalk on the zero drift and random walk of fiber optic gyroscope[J]. *Acta optica sinica*, 2014, 34(12): 14-24.
- [15] FENG T, DING D, LI Z, et al. First quantitative determination of birefringence variations induced by axial-strain in polarization maintaining fibers[J]. *Journal of lightwave technology*, 2017, 35(22): 4937-4942.
- [16] DING Z, MENG Z, YAO X S, et al. Accurate method for measuring the thermal coefficient of group birefringence of polarization-maintaining fibers[J]. *Optics letters*, 2011, 36(11): 2173-2175.
- [17] CHUA T H, CHEN C L. Fiber polarimetric stress sensors[J]. *Applied optics*, 1989, 28(15): 3158-3165.
- [18] TANG F, JING W C, ZHANG Y M, et al. Measurement of distributed mode coupling in high birefringence polarization-maintaining fiber with random polarization modes exited[C]//ICO20: Optical Information Processing, January 20, 2006, Changchun, China. Bellingham: SPIE, 2006: 165-174.